JACS
JOURNAL OF THE AMERICAN CHEMICAL SOCIETY
Article
pubs.acs.org/JACS

Profiling Genome-Wide Chromatin Methylation with Engineered Posttranslation Apparatus within Living Cells

Rui Wang,[†,‡,§] Kabirul Islam,[†,§] Ying Liu,[∥] Weihong Zheng,[†] Haiping Tang,[⊥] Nathalie Lailler,[#] Gil Blum,[†,¶] Haiteng Deng,[⊥] and Minkui Luo*[,†]

[†]Molecular Pharmacology and Chemistry Program, Memorial Sloan-Kettering Cancer Center, New York, New York 10065, United States

[‡]Program of Pharmacology, Weill Graduate School of Medical Science, Cornell University, New York, New York 10021, United States

[∥]Program of Biochemistry & Structural Biology, Cell & Developmental Biology, and Molecular Biology, Weill Graduate School of Medical Science, Cornell University, New York, New York 10021, United States

[⊥]School of Life Sciences, Tsinghua University, Beijing, 100084 China

[#]Genomics Core Laboratory, Memorial Sloan-Kettering Cancer Center, New York, New York 10065, United States

[¶]Tri-Institutional Training Program in Chemical Biology, Memorial Sloan-Kettering Cancer Center, New York, New York 10065, United States

Supporting Information

ABSTRACT: Protein methyltransferases (PMTs) have emerged as important epigenetic regulators in myriad biological processes in both normal physiology and disease conditions. However, elucidating PMT-regulated epigenetic processes has been hampered by ambiguous knowledge about *in vivo* activities of individual PMTs particularly because of their overlapping but nonredundant functions. To address limitations of conventional approaches in mapping chromatin modification of specific PMTs, we have engineered the chromatin-modifying apparatus and formulated a novel technology, termed clickable chromatin enrichment with parallel DNA sequencing (CliEn-seq), to probe genome-wide chromatin modification within living cells. The three-step approach of CliEn-seq involves *in vivo* synthesis of *S*-adenosyl-L-methionine (SAM) analogues from cell-permeable methionine analogues by engineered SAM synthetase (methionine adenosyltransferase or MAT), *in situ* chromatin modification by engineered PMTs, subsequent enrichment and sequencing of the uniquely modified chromatins. Given critical roles of the chromatin-modifying enzymes in epigenetics and structural similarity among many PMTs, we envision that the CliEn-seq technology is generally applicable in deciphering chromatin methylation events of individual PMTs in diverse biological settings.

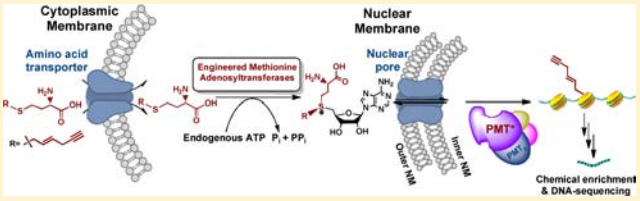

INTRODUCTION

Enzymatic transfer of the methyl group from the cofactor *S*-adenosyl-L-methionine (SAM) to DNA, RNA, protein and metabolite substrates accounts for the repertoire of biologically relevant methylation.[1] As an important subtype, protein posttranslational methylation increases functional diversity of proteome and thus influences numerous aspects of normal cell biology.[2] In contrast, misregulation of these events has been implicated in many diseases including developmental disorders and cancer.[2] The human genome encodes more than 60 protein methyltransferases (PMTs), and their epigenetic functions are mainly executed via methylating diverse histone and nonhistone targets.[3]

PMT-mediated histone methylation, together with other chromatin events such as DNA methylation and ATP-dependent chromatin remodeling, establishes specific chromatin states for gene regulation, chromosome recombination and DNA repair.[4,5] To elucidate biological roles of individual PMTs on these chromatin events, it is critical to define their genome-wide chromatin modification sites in an unambiguous manner. However, considerable challenge exists for conventional approaches to define such sites for a single PMT because PMTs often harbor overlapping chromatin-modifying activities (e.g., the methylation of histone H3 lysine 9 by G9a, GLP1, SETDB1/2, SUV39H1/2 and PRDM2).[6−9] Moreover, dynamic chromatin modifications often need to be executed via multiple cellular machineries within living cells.[4] To address these challenges in deciphering the activities for individual PMTs in chromatin landscape, we envisioned an approach suitable for the in-cell setting.

In living cells, a native methylation reactome consists of two crucial enzymatic reactions (Figure 1): SAM biosynthesis and substrate labeling. The biosynthesis of SAM **2a** from methionine **1a** and adenosine triphosphate (ATP) is carried out by methionine adenosyltransferases (MATs).[10] Here we

Received: September 22, 2012
Published: December 17, 2012

© 2012 American Chemical Society

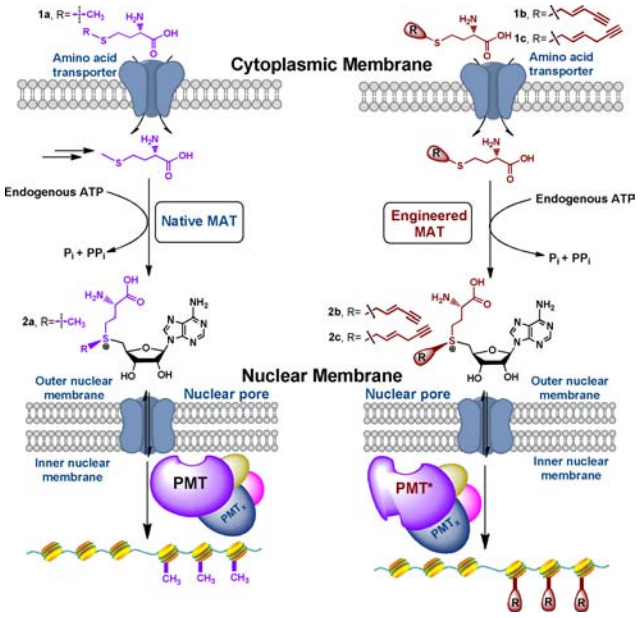

Figure 1. Schematic description of profiling genome-wide chromatin methylation with a native or engineered posttranslation apparatus within a living cell. In a native context, methionine **1a** and adenosine triphosphate (ATP) will be processed by methionine adenosyltransferases (MAT) into SAM **2a**. SAM then serves a methyl donor cofactor of PMTs. In contrast, a methionine analogue (e.g., Hey-Met **1c**) can penetrate into cells and then be processed by an engineered MAT to generate the corresponding SAM analogue *in situ*. The SAM analogue serves a cofactor surrogate of engineered PMTs (PMT*) for bioorthogonal labeling of substrates.

envisioned in-cell-based mapping of chromatin methylation using an engineered posttranslation reactome. This approach is featured by using an engineered methionine adenosyltransferase (MAT) within living cells to process membrane-permeable methionine analogues into SAM analogues, which themselves show limited cell-permeability.[11] The in-cell-produced SAM analogues can then be utilized *in situ* by compatible PMT variants to label chromatin with distinct chemical handles for target enrichment and characterization (Figure 1).

G9a (EuHMT2/KMT1C) and GLP1 (EuHMT1/KMT1D) are two human oncogenic protein lysine methyltransferases (PKMTs) with their epigenetic functions implicated in silencing viral genes and tumor suppressors.[12] G9a and GLP1, together with other H3K9 PMTs (e.g., SUV39H1, SETDB1 and PRDM2), methylate H3 lysine 9 (H3K9) via multimeric complexes in cellular contexts.[6−9] Dissecting chromatin-modifying activities of these H3K9 PMTs is challenging but important toward elucidating their physiological and pathogenic functions. With G9a and GLP1 as representative PMTs, we demonstrated the use of methionine analogues, a MAT variant and engineered PMTs for substrate labeling *in vitro* and genome-wide chromatin modifications within living cells.

RESULTS AND DISCUSSION

Engineering MATs for Enzymatic Synthesis of SAM Analogues *in Vitro*. In the course of developing *in vitro* approaches to profile protein methylation, terminal alkyne-containing (*E*)-pent-2-en-4-ynyl-SAM (EnYn-SAM, **2b**) and (*E*)-hex-2-en-5-ynyl-SAM (Hey-SAM, **2c**) have been characterized as active cofactors of G9a's Y1154A mutant and used to label G9a's targets *in vitro*.[13] To transform the approach to living cells, we first examined the feasibility of MAT-mediated chemoenzymatic synthesis of the two SAM analogues from the corresponding methionine analogues.

In a biological setting, SAM is synthesized from endogenous ATP and cell permeable methoinine by highly conserved MATs.[14,15] Upon analyzing the structures of MATs (PDB code 1RG9 for *Escherichia coli* MAT[10] and PDB code 2P02 for human MAT2A), we noticed the existence of a highly conserved small methylthio-binding pocket formed by hydrophobic I117, G120, V121 and I322 residues (the sequence number of human MAT2A, Figure 2a). To expand the pocket

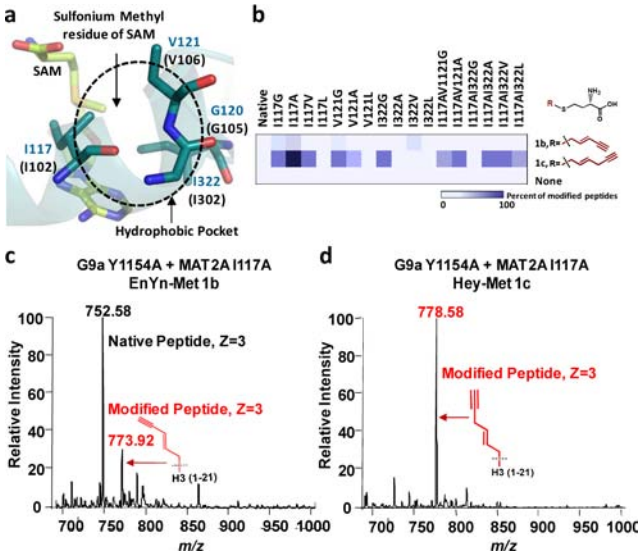

Figure 2. Engineering MAT2A for chemoenzymatic synthesis of SAM analogues. (a) Key residues consisting of the hydrophobic methylthio-binding pocket in *E. coli* MAT (PDB 1RG9) and human MAT2A (PDB 2P02). The backbone structure was constructed on the basis of *E. coli* MAT. The key residues (I117, G120, V121 and I322) were labeled with cyan for human MAT2A and black for *E. coli* MAT. (b) Heat map analysis of *in vitro* activities of MAT2A mutants on methionine analogues. Human MAT2A mutants were coupled with the G9a Y1154A in the reactome containing H3K9 peptide, ATP and the methionine analogue (**1b** or **1c**). (c, d) Representative LC−MS of the resultant modified histone H3 peptide (presented as modification %) from the *in vitro* coupling reactomes. (c) Mass spectrum of EnYn-Met **1b** and MAT2A I117A coupled with G9a Y1154A mutant. (d) Mass spectrum of Hey-Met **1c** and MAT2A I117A coupled with G9a Y1154A mutant (see Figure S1 in the Supporting Information for MS data of all mutants).

to accommodate bulky methionine analogues such as *S*-(*E*)-pent-2-en-4-ynyl and *S*-(*E*)-hex-2-en-5-ynyl homocysteine (EnYn-Met **1b** and Hey-Met **1c**, Figures 1, 2b, Experimental Section and Supporting Information), the I117, V121 and I322 residues were systemically replaced with smaller amino acids (Ala, Gly, Leu or Val) individually or in a combination manner. The active MAT2A variants were identified upon coupling with G9a's Y1154A mutant and then detecting the anticipated alkylation product in the presence of ATP and EnYn-Met **1b** or Hey-Met **1c**. Among the 17 examined MAT2A mutants, the I117A variant has the best activity toward EnYn-Met **1b** and Hey-Met **1c** as shown by its highest alkylation efficiency (30% for **1b** and 100% for **1c**, Figure 2b−d, Figure S1 in the Supporting Information). In contrast, native MAT2A and other mutants are either inert or slightly active toward the methionine

analogues (Figure 2b, Figure S1 in the Supporting Information). The general preference of Hey-Met **1c** over EnYn-Met **1b** revealed in the two-enzyme coupled assays might be attributable to the higher activities of the MAT2A variant on Hey-Met **1c** or the G9a mutant on Hey-SAM **2c**, which will be examined elsewhere. Here the efficient conversion of Hey-Met **1c** into Hey-SAM **2c** by the I117A mutant presents the MAT2A variant as a suitable component to construct a bioorthogonal posttranslation apparatus.

Generality of engineered MATs Coupled with PMT Variants for *in Vitro* Substrate Labeling. To examine the generality of the MAT2A I117A mutant, we explored whether the MAT variant is compatible with other PMT variants. G9a-like protein 1 (GLP1) is a human protein lysine methyltransferase, which also acts on H3K9.[12] The SAM-binding motif of GLP1 can be tailored (GLP1-Y1211A) to incorporate the bulky SAM analogue Hey-SAM **2c** (manuscript in revision). Besides PKMTs, protein arginine methyltransferase 1 (PRMT1), the predominant mammanlian type 1 PRMT,[16] was also successfully engineered, and its Y39FM48G variant has been shown to be active toward another SAM analogue 4-propargyloxy-but-2-enyl-SAM (Pob-SAM).[17] Upon coupling the GLP1 variant with the MAT2A I117A mutant in the presence of Hey-Met **1c** and ATP, a robust alkylation of GLP1's H3K9 peptide substrate was observed (Figure S1 in the Supporting Information). In a similar manner, the MAT2A I117A mutant can process *S*-4-propargyloxy-but-2-enyl homocysteine (Pob-Met) into Pob-SAM and, upon coupling with the PRMT1 Y39FM48G mutant, can label the PRMT1 substrate RGG peptide (here Pob-SAM but not Hey-SAM **2c** was found to be an active cofactor of the PRMT1 mutant *in vitro*[17]) (Figure S2 in the Supporting Information). The coupled activities of the MAT mutant and the engineered G9a/GLP1 variants were also validated with the full-length H3, an *in vivo* protein substrate of G9a and GLP1.[6] Tandem MS of the tryptic H3 peptides confirmed the expected (*E*)-hex-2-en-5-ynylation on H3K9, the known methylation site of the two PMTs (Figure S3 in the Supporting Information). The MAT2A I117A variant thus demonstrated the robust compatibility with multiple bulky methionine analogues and engineered PMTs for *in situ* generation of SAM analogues.

Biosynthesis of SAM Analogues within Living Cells. SAM analogues show poor membrane permeability and thus are restricted for the access to intracellular PMTs.[11] In addition, chemically synthesized SAM analogues consist of diastereomeric mixtures with only the sulfonium-(*S*)-epimer bioactive.[14] To circumvent these limitations, we envision that, in the presence of the engineered MAT in living cells, pure bioactive SAM analogues can be produced *in situ* from the corresponding membrane-permeable methionine analogues. With the MAT2A I117A variant characterized above, we investigated its activity to process Hey-Met **1c** into Hey-SAM **2c** in living cells. Here the MAT2A I117A mutant was expressed in human embryonic kidney 293T (HEK293T) cells followed by the supply of Hey-Met **1c** in a methionine-free growth medium. Hey-SAM **2c** was readily extracted from the cell pellets (Figure 3a) and confirmed by MS (Figure S5 in the Supporting Information), consistent with the intracellular production and maintenance of Hey-SAM **2c**. Hey-SAM's in-cell biosynthesis was further confirmed by the dose-dependent increase of intracellular Hey-SAM **2c**, which reaches a plateau around 1 mM Hey-Met **1c** (ESI-MS, Figure 3a,b, Figure S5 in the Supporting Information). In contrast, no Hey-SAM **2c** was detected

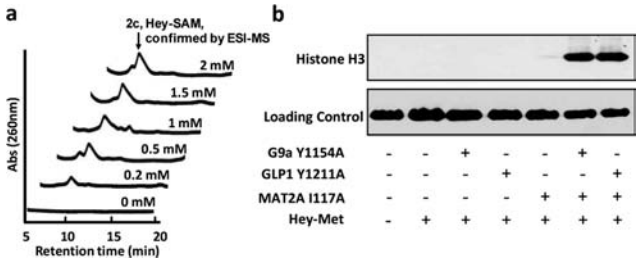

Figure 3. Biosynthesis of Hey-SAM **2c** and Hey-SAM-mediated histone alkylation within living cells. (a) Production of Hey-SAM **2c** within living cells. HEK293T cells were transfected with the MAT2A I117A and supplied with various concentrations of Hey-Met **1c**. The resultant production of Hey-SAM **2c** was detected by HPLC and confirmed by MS (see data in panel b). (b) Enrichment of (*E*)-hex-2-en-5-ynylated histone H3. HEK293T cells were cotransfected with the G9a/GLP1 Y1154A/Y1211A and MAT2A I117A mutants. After incubating HEK293T cells with 1 mM Hey-Met **1c** under a methionine-depleted medium, the resultant modified proteins were acid-precipitated and conjugated with the azido−diazo−biotin probe, enriched with streptavidin beads, and then blotted with anti-H3 antibody blotting (the upper panel). The controls without Hey-Met **1c**, engineered PMTs or MAT2A were also included. See Figure S4b in the Supporting Information for the controls with native MAT, G9a or GLP. The loading control is shown in the lower panel.

when cells were transfected with native MAT2A or grown in the absence of Hey-Met **1c** (Figure 3a, Figure S4a in the Supporting Information), emphasizing the roles of the MAT2A I117A mutant and Hey-Met **1c** for intracellular production of Hey-SAM **2c**.

To examine the efficiency of engineered MAT2A to produce Hey-Met **1c** within living cells, we quantified the amount of intracellular Hey-SAM **2c** by LC/MS (see Experimental Section for details). The presence of 1 mM Hey-Met **1c** in the growth medium led to the intracellular accumulation of approximately 4.7 nmol of Hey-SAM/10^6 cells, which is comparable with the reported amount of SAM in cells (~5 nmol of SAM/10^6 cells).[18] Moreover, the toxicity of Hey-Met **1c** was evaluated with the Alamar blue assay. The presence of <2 mM Hey-Met **1c** has no obvious effect on the viability of HEK293T cells. When the cells were transfected with the MAT2A I117A plasmid, only slight growth inhibition (~15% compared to control) was observed in the presence of Hey-Met **1c** (Figure S7 in the Supporting Information). These findings suggest that neither Hey-Met **1c** nor Hey-SAM **2c** has significant cellular toxicity under the examined concentrations. These results collectively argue that Hey-Met **1c** can penetrate through cell membranes and, together with endogenous ATP, be processed into Hey-SAM **2c** by the MAT2A I117A variant within living cells. The intracellular production of the SAM analogue thus circumvents its membrane permeability issue,[11,14] and enables its utility within living cells.

Using Engineered Methylation Apparatus To Label Targets of G9a and GLP1 within Living Cells. Given that both G9a's Y1154A mutant and GLP1's Y1211A mutant can process Hey-SAM **2c** *in vitro* for substrate labeling, we then constructed the engineered posttranslation apparatus within living cells by coexpressing the MAT2A I117A variant with the two PMT mutants, respectively. After growing the cells in the presence of Hey-SAM's biosynthetic precursor Hey-Met **1c** (1 mM), cell lysates were subjected to the click chemistry with a cleavable azido−diazo−biotin probe (see Experimental Section and Supporting Information and the protocol below for

profiling genome-wide chromatin modification).[19] The putative (*E*)-hex-2-en-5-ynylated proteins were enriched with streptavidin beads, cleaved from streptavidin beads after washing and then blotted with anti-H3 antibody (Experimental Section and Supporting Information). Histone H3 was pulled down only from the samples containing the engineered MAT, the PMT variants and Hey-Met, consistent with the *in vivo* activity of native G9a and GLP1 on histone H3. In contrast, no labeling was observed for the controls that lack any of the three components or were transfected with native MAT, G9a or GLP (Figure 3b, Figure S4c in the Supporting Information), indicating the prerequisite of the engineered components (MAT/G9a/GLP1 variants and the matched Met analogues) for the bioorthogonal target labeling within living cells. To further verify that the PMT variants, like native G9a and GLP1, act on H3K9 within living cells, the total histones were acid-precipitated and analyzed by LC−MS/MS. The desired (*E*)-hex-2-en-5-ynylation on lysine 9 in histone H3 demonstrated that the engineered apparatus recapitulates the activities of native G9a and GLP1 for target labeling within living cells (Figure S6 in the Supporting Information).

To examine the efficiency of the engineered methylation apparatus, we implemented this method to probe the time-dependent global methylation activity of G9a within living cells. The cells were transfected with the MAT2A I117A and G9a Y1154A mutants and then treated with Hey-Met **1c** (1 mM) for a varied period of time. The cell lysates were recovered and reacted with an azido fluorescent dye via copper-catalyzed azide−alkyne cycloaddition (CuAAC) reaction, followed by visualization with in-gel fluorescence. As revealed previously that G9a acts on histone and diverse nonhistone targets,[29] the labeling of G9a targets can be readily observed after 8 h treatment of Hey-Met **1c** to the cells carrying the engineered MAT2A and G9a mutants. In contrast, only marginal background labeling was observed in the cells transfected with the MAT2A I117A mutant alone (Figure S9 in the Supporting Information), arguing the importance of the presence of the engineered G9a for the targeting labeling. The background labeling might be due to residual activities of certain native PMTs on Hey-SAM **2c**. Given that histone demethylases have high specificity for substrates,[20,21] the bulky (*E*)-hex-2-en-5-ynylated proteins may not be substrates of wild type demethylases and thus resistant to dealkylation. The issues of the background and stability of the (*E*)-hex-2-en-5-ynylated proteins remain to be addressed with additional experiments.

Profiling Genome-Wide Chromatin-Modifying Activities of G9a and GLP1. With the feasibility to construct the in-cell-based bioorthogonal posttranslation apparatus, we further leveraged the system to examine genome-wide chromatin-modifying activities of G9a and GLP1 via an unprecedented approach, termed as clickable chromatin enrichment with parallel DNA sequencing (CliEn-seq). Here the (*E*)-hex-2-en-5-ynylated chromatins, generated by the engineered MAT2A and G9a/GLP within the living cells supplied with Hey-Met **1c**, were further conjugated to the cleavable azido−diazo−biotin probe via CuAAC,[19] followed by affinity pull-down with streptavidin beads (Figure 4a). We observed the 30−50-fold enrichment of chromatin DNA from the cells cotransfected with engineered MAT2A I117A and G9a Y1154A/GLP1 Y1211A in contrast with the control group transfected with the MAT2A I117A mutant alone (Figure 4b). To resolve the gene loci containing the (*E*)-hex-2-en-5-ynylated chromatins, the enriched chromatin DNA was subjected to next-generation sequencing. The CliEn-seq data suggest that the activity of G9a is broadly spread around genome-wide chromatins in HEK293T cells including the previously known G9a-targeted loci *myoD, rb1* and *bmi1* (Figure 4c, Figure S10 in the Supporting Information).[22,23] The enriched activity of G9a

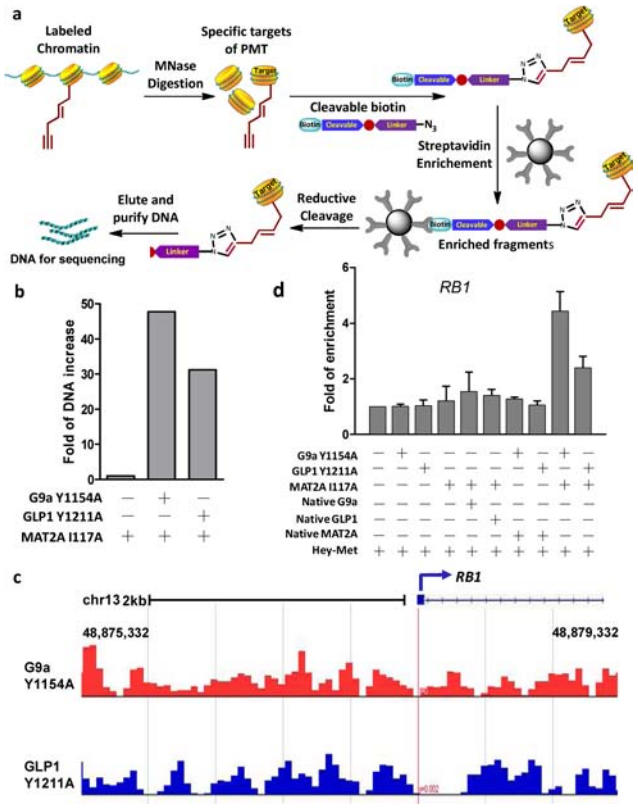

Figure 4. Profiling genome-wide chromatin modification of G9a and GLP1. (a) Schematic description of clickable chromatin enrichment with parallel DNA sequencing (CliEn-seq). Here the terminal-alkyne-modified chromatins were conjugated with the cleavable azido−diazo−biotin probe, followed by enrichment with streptavidin beads, the cleavage, and then DNA sequencing. The positive data of CliEn-seq were then validated with quantitative PCR (CliEn-qPCR). (b) DNA enrichement for CliEn-seq analysis. DNA was recovered from the same number of cells transfected with MAT2A I117A and G9a/GLP1 Y1154A/Y1211A mutants. The DNA amount (after normalizing to the input DNA amount) is presented as the fold of DNA increase versus the control, which was transfected with the MAT2A I117A mutant alone. The samples typically showed ∼30−50-fold enrichment of DNA compared to the control group. (c, d) CliEn-seq and qPCR validation of a representative gene harboring the enriched activities of G9a/GLP1. (c) CliEn-Seq showed the levels of the (*E*)-hex-2-en-5-ynylation at the *RB1* gene in HEK293T cells (see Figure S10 in the Supporting Information for *MYOD* and *BMI1*). The CliEn-seq files were normalized by the total reads and processed in Genplay tool. Red: cells cotransfected with the MAT2A and G9a mutants in the presence of Hey-Met. Blue: cells cotransfected with the MAT2A and GLP1 mutants in the presence of Hey-Met. (d) Representative CliEn-qPCR validation of the (*E*)-hex-2-en-5-ynylation at the promoter and gene body of *RB1* (see Figure S10 in the Supporting Information for *MYOD* and *BMI1*). The same sets of experiments were carried out for actin promoter as the control loci in the absence of G9a or GLP1 (Figure S10 in the Supporting Information). CliEn-qPCR signals are normalized as the fold of enrichment to the negative control without the engineered MAT2A, G9a or GLP1 variants. Controls with wild type enzymes (MAT2A, G9a and GLP1) were also included. Error bars represent means ± SEM (n = 3).

at these representative loci was independently confirmed by qPCR (CliEn-qPCR, Figure 4d, Figure S10 in the Supporting Information).

G9a and GLP1 were proposed to account for the activities of methylating histone H3 (H3K9me2) and nonhistone targets, respectively.[24] Remarkably, our CliEn-seq and CliEn-qPCR data showed that G9a and GLP1 harbor complementary chromatin-modifying activities at the loci, which were previously known to be G9a targets (Figure 4c,d, Figure S10 in the Supporting Information). This finding is also consistent with our chromatin immunoprecipitation (ChIP) experiment using anti-H3K9me2 antibody, where overexpressing either G9a or GLP1 enhanced the H3K9me2 marker on the targeted promoters of the examined genes (Figure S10 in the Supporting Information). To further distinguish the activities of G9a/GLP1 between the promoter regions and gene bodies, we selected 35 gene loci known to contain H3K9 methylation sites (Table S2 in the Supporting Information) and dissected the CliEn-seq data of the (*E*)-hex-2-en-5-ynylation pattern according to their transcription start sites (TSS) and transcription end sites (TES). The comparable enrichment of the G9a- or GLP1-mediated (*E*)-hex-2-en-5-ynylation across TSS and TES suggests that G9a and GLP1 have no significant preference between the gene promoters and the gene bodies in HEK293T cells (Figure 5). The CliEn-seq approach using the engineered posttranslation system thus enables the deciphering of the activities of closely related PMTs within living cells.

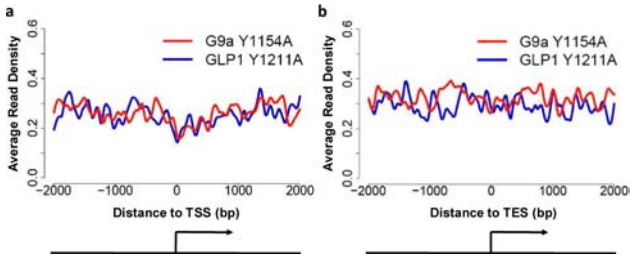

Figure 5. CliEn-seq signal enrichment profile near the transcription start site (TSS) (a) and the transcription end site (TES) (b) for 35 selected genes with known H3K9 methylation markers (see Supporting Information for the list of the genes). Red: the sample cotransfected with the MAT2A I117A and G9a Y1154A mutants. Blue: the sample cotransfected with the MAT2A I117A and GLP1 Y1211A mutants. Arrow: the direction of transcription. *X*-axis: the distance to TSS/TES. *Y*-axis: the average read density.

CONCLUSION

Since the first human protein methyltransferase SUV39H1 was reported, tremendous efforts have been made in defining new PMTs and their biological functions.[25,26] While such studies led to understanding biochemical functions of PMTs *in vitro*, the precise description of genome-wide chromatin-modifying sites of individual PMTs is lacking.[4] Here we have addressed such need via reconstructing bioorthogonal posttranslation apparatus within living cells with engineered MAT and PMTs. The engineered reactomes can efficiently process membrane-permeable methionine analogues into SAM analogues within living cells and then label chromatins *in situ*. The advantage of developing such a bioorthogonal system is to harness the specificity of genetic technique in generating a PMT variant that would only act on SAM analogue but not native SAM, thus providing a means for functional analysis of a specific PMT in cells. While the bioorthogonal approach has been successfully applied to other classes of enzymes, here we have demonstrated that multiple enzymes in a common biochemical pathway can be engineered to sequentially generate and utilize cofactor analogues from corresponding precursor analogues in living cells.

The terminal-alkyne handle of the SAM analogues further allowed the modified chromatins to be enriched with the azido-containing biotin probe and then mapped with DNA sequencing technologies (CliEn-seq or CliEn-qPCR). In comparison with conventional ChIP-seq (chromatin immunoprecipitation with parallel DNA sequencing) experiments,[27] which cannot distinguish chromatin-modifying activities of closely related enzymes (e.g., all the H3K9 PMTs), the merit of CliEn-seq lies in its ability to trace chromatin-modifying activities of a designated single PMT in an unambiguous manner. Here we demonstrated one application of CliEn-seq by dissecting the activities of closely related G9a and GLP1 (and likely PRMT1 as well) and showed that the two PMTs have complementary H3K9 methylation activities across TSS and TES of target genes in HEK293T cells.

Extensive structural and biochemical investigations have led to the identification of conserved structural motifs of PMTs and suggest a common mechanism for cofactor recognition and catalysis. Given that multiple PMTs can be engineered to process bulky SAM analogues for target labeling,[13,17] the corresponding engineered apparatuses are expected to be readily coupled with the MAT2A variant. The resultant constructed posttranslation apparatus can be applied to map genome-wide chromatin-modifying sites within living cells. More importantly, the promiscuous MAT variants and the corresponding methionine analogues developed here can be coupled with other methyltransferases for target labeling.[28] The present work thus documents a powerful approach and the corresponding reagents to reveal downstream readouts of diverse PMTs.

EXPERIMENTAL SECTION

Synthesis, Purification and Characterization of *S*-(Pent-2-en-4-yny)-L-homocysteine (EnYn-Met, 1b), *S*-(Hex-2-en-5-yny)-L-homocysteine Trifluoroacetic Salt (Hey-Met, 1c), and *S*-[4-(Prop-2-ynyloxy)but-2-enylthio]-L-homocysteine (Pob-Met). *S*-Benzyl-L-homocysteine (255 mg, 1 mmol) was placed in a round-bottom flask connected to an ammonia cylinder. Into the flask with a dry ice−ethanol bath was added liquid ammonia (20 mL). Sodium metal (50 mg, 2.2 mmol) was then added portionwise (from a clear solution to a dark blue solution). Within a few minutes, the solution became colorless. The dry ice−ethanol bath was removed to allow the evaporation of ammonia. The remaining trace of ammonia was removed with the aid of a flow of argon, followed by vacuum. The resulting white solid was dissolved in dry ethanol (10 mL) and cooled to 0 °C. A solution of (*E*)-6-bromohex-4-en-1-yne, (*E*)-pent-2-en-4-ynyl tosylate or (*E*)-1-bromo-4-(prop-2-ynyloxy)but-2-ene (1.05 mmol) in ethanol (3 mL) was added (see Supporting Information for the synthesis of these precursors). This reaction mixture was stirred at 0 °C for 1 h, followed by overnight at ambient temperature (22 °C). The ethanol was removed under reduced pressure. The resultant mixture was redissolved in distilled deionized (DD) water (5 mL) and passed through a Dowex 50 (H^+) ion-exchange column. The column was washed with DD water until neutral and then eluted with diluted ammonia hydroxide (5% DD water solution). The portions containing the expected products (monitored by silica gel TLC eluted with 4:1:1 v/v/v *n*-BuOH/AcOH/H_2O and detected by 0.2% ninhydrin in 16:3:1 v/v/v 96% EtOH/AcOH/*s*-collidine upon heating) were combined and concentrated on a rotary evaporator to yield white solids. The crude products were then dissolved in 0.1 N HCl and subjected to

further purification with the preparative reversed-phase HPLC (XBridge Prep C18 5 μm OBD 19 × 150 mm). The final products were eluted with linear gradients from 10% to 60% of acetonitrile containing 0.1% trifluoroacetic acid in aqueous trifluoroacetic acid (0.1%) in 15 min with a flow of 10 mL/min. The desired fractions were collected and lyophilized to yield white powders (yields of 56%, 35% and 58% of **1b**, **1c** and Pob-Met, respectively).

^{1}H NMR for EnYn-Met **1b** (500 MHz, D_2O + formic acid-d_2): δ 1.98−2.04 (m, 1H), 2.06−2.12 (m, 1H), 2.50 (t, 2H, J = 7.4 Hz), 3.12 (d, 2H, J = 7.4 Hz), 3.15 (s, 1H), 3.99 (t, 1H, J = 6.0 Hz), 5.50 (d, 1H, 15.7 Hz), 6.06−6.12 (m, 1H). ^{13}C NMR (125 MHz, D_2O + formic acid-d_2): δ 25.99, 30.15, 33.06, 52.86, 79.09, 82.71, 111.45, 142.06, 172.77. MS(ESI) m/z: 200 $[M + H]^+$. HRMS: calculated for $C_9H_{14}NO_2S$ ($[M + H]^+$) 200.0745, found 200.0746.

^{1}H NMR for Hey-Met **1c** (500 MHz, D_2O): 2.13−2.19 (m, 1H), 2.22−2.28 (m, 1H), 2.52 (t, 1H, J = 2.6 Hz), 2.66 (t, 2H, J = 7.5 Hz), 3.00−3.02 (m, 2H), 3.23 (dd, 2H, J = 7.2, 0.7 Hz), 4.14 (t, 1H, J = 6.3 Hz), 5.64−5.70 (m, 1H), 5.75−5.81 (m, 1H). ^{13}C NMR (150 MHz, D_2O + formic acid-d_2): δ 21.20, 25.68, 30.14, 32.68, 52.78, 71.94, 83.23, 117.00 (q, J = 289.78), 127.90, 128.37, 163.65 (q, J = 35.2 Hz), 172.76. MS(ESI) m/z: 214 $[M + H]^+$. HRMS: calculated for $C_{10}H_{16}NO_2S$ ($[M + H]^+$) 214.0902, found 214.0898.

^{1}H NMR for Pob-Met (500 MHz, DMSO-d_6): 1.74−1.82 (m, 1H), 1.93−1.99 (m, 1H), 2.54 (t, 1H, J = 7.6 Hz), 3.15 (d, 2H, J = 5.8 Hz), 3.20−3.33 (m, 1H), 3.45 (d, 1H, J = 2.4 Hz), 3.98 (d, 2H, J = 4.3 Hz), 4.12 (d, 2H, J = 2.4 Hz),5.64−5.67 (m, 2H), 7.54 (brs, 2H). ^{13}C NMR (150 MHz, DMSO-d_6): δ 26.62, 31.06, 32.04, 53.14, 56.53, 68.79, 77.27, 80.32, 128.38, 129.49, 169.15. MS(ESI) m/z: 244 $[M + H]^+$. HRMS: calculated for $C_{11}H_{17}NO_3NaS$ ($[M + Na]^+$) 266.0827, found 266.0822.

Bacterial Expression and Purification of Proteins. Full-length human MAT2A plasmid was provided by Dr. Udo Oppermann at University of Oxford. The N-terminal His_6-tagged human MAT2A in a pNIC28-Bsa4 kanamysin-resistant vector (http://www.sgc.ox.ac.uk/structures/MM/MAT2AA_2p02_MM.html) was expressed in *E. coli* (DE3) Rosseta 2 strain. A single colony was inoculated into 5 mL of Miller Luria−Bertani (LB) medium containing 50 μg/mL kanamycin and 34 μg/mL chloramphenicol and grown at 37 °C overnight. Ten milliliters of the o/n culture was added into 1 L of LB medium, and the resultant medium was allowed to grow at 37 °C until OD_{600} = 0.6−0.8. The cells were then induced with 0.5 mM IPTG at 17 °C for another 16 h before harvesting. The cell pellets were collected and homogenized by French press cell disruptor (Thermo) in lysis buffer (50 mM Tris-HCl, pH = 8.0), 50 mM NaCl, 5 mM β-mercaptoethanol, 25 mM imidazole, Roche protease inhibitor and 5% (v/v) glycerol. After centrifuging at 15000g for 1 h at 4 °C, MAT2A was purified by Ni-NTA agarose resin (Qiagen) according to the previous method,[17] followed by a 5 mL HiTrap-Q Sepharose XL column (GE healthcare) using a linear gradient from 35 mM to 1 M KCl in a buffer containing 25 mM Tris-HCl (pH = 8.0) and 5% (v/v) glycerol. Fractions containing MAT2A were combined and concentrated using an Amicon Ultra-10K centrifugal filter device. The protein concentrations were determined with a Bradford assay kit (BioRad) with BSA as a standard. The concentrated proteins were stored at −80 °C prior to use. All MAT2A mutants were generated by using QuickChange site-directed mutagenesis kit (Stratagene) according the vendor's protocols. The resulted mutant plasmids were confirmed by DNA sequencing. The mutants were expressed and purified as described above for the native protein. The G9a/GLP1 mutants and 5′-methylthioadenosine nucleosidase (MTAN) were expressed and purified as described previously.[3−5]

Mass Spectrometric Assays of *in Vitro* Coupled Reactions of MAT2A and PMT Variants. For the reactions using histone peptide as the substrate, 50 μM H3 (1−21) peptide was added into 100 μL of a mixture containing 50 mM Tris-HCl (pH 8.5), 100 mM KCl, 2 mM $MgCl_2$, 2.5 mM ATP, 2.5 mM methionine analogue, 7.5 μM MAT2A mutant, 1 μM G9a or GLP1 mutant and 20 nM MTAN. The resultant reaction mixture was incubated for 10 h at ambient temperature (22 °C). For the reactions using RGG peptide as the substrate, 50 μM RGG peptide substrate was added into 100 μL of a mixture containing 50 mM Tris-HCl (pH = 8.5), 100 mM KCl, 2 mM $MgCl_2$, 2.5 mM ATP, 2.5 mM methionine analogues, 7.5 μM MAT2A mutant, 2 μM PRMT1 mutant and 20 nM MTAN. The resultant reaction mixture was incubated for 10 h at ambient temperature (22 °C). The samples were then concentrated to around 20 μL by a SpeedVac and injected into LC−MS for analysis according to the previously described protocols.[13,17,29]

For the reactions with histone substrate, 10 μM recombinant human histone H3 (New England Biolab) was added into 100 μL of a mixture containing 50 mM Tris-HCl (pH = 8.5), 100 mM KCl, 2 mM $MgCl_2$, 2.5 mM ATP, 2.5 mM methionine analogue, 7.5 μM MAT2A mutant, 1 μM G9a or GLP1 mutant and 20 nM MTAN. The resultant reaction mixture was incubated for 24 h at ambient temperature (22 °C). The histone-containing reaction samples were passed through a Sep-Pak Vac C18 1 cm^3 column (Waters, Milford, MA). The protein mixture was then eluted with 1:1 acetonitrile and 0.1% TFA, concentrated with a SpeedVac and resolved by SDS−PAGE (Criterion Precast gel, 18% Tris-HCl, Bio-Rad) followed by staining with Coomassie Blue (Bio-Rad). The corresponding histone H3 gel bands were subjected to LC−MS/MS analysis according to the method described previously.[13,17,29]

Cloning and Mutagenesis of Mammalian Vectors. Full-length N-terminal flag-tagged human MAT2A was constructed by PCR using pNIC28-Bsa4-MAT2A (provided by Dr. Udo Oppermann at University of Oxford) as the template. The following primers were used: 5′-GATTAGAATTCATG**GACTACAAAGACGATGACGATAAA**AACGGACAGCTCAACGGCTTCCAT-3′ (forward with the Flag tag sequence in bold); 5′-TAATCCTCGAGTCAATATTTAAGCTTTTTGGGCACTTCCCATGGGAAGCTGTC-3′ (reverse). The resultant PCR product was cloned into pcDNA3 vector through *Eco*RI/*Xho*I restrictive sites to yield the pcDNA3-Flag-MAT2A plasmid. The I117A variant of pcDNA3-Flag-MAT2A plasmid was generated with the pcDNA3-Flag-MAT2A plasmid as the template with Quick change site-directed mutagenesis kit (Stratagene) according to the manufacturer's instruction. The plasmids of pcDNA3-Flag-G9a/GLP1 and their variants were constructed as described previously.[29]

Transfection of G9a/GLP1/MAT2A Variants Followed by the Treatment of Methionine Analogues. HEK293T cells (ATCC) were cultured in Dulbecco's modified Eagle medium (DMEM) with 10% (v/v) fetal bovine serum (FBS) and maintained in a humidified incubator at 37 °C and 5% CO_2. The cells were seeded into CellBIND surface T75 flask (Corning) and transiently transfected with G9a/GLP1/MAT2A plasmids (native or mutants) in Lipofectamine 2000 (Invitrogen) at 30−40% confluence according to the manufacturer's instructions. The cells were washed with PBS 12 h after transfection and recovered in fresh DMEM medium for 24 h. The medium was then removed, and the cells were incubated in methionine-deficient DMEM medium (Invitrogen) supplemented with 10% dialyzed FBS (Gibco) for 30 min in the CO_2 incubator to deplete the intracellular methionine. The medium was then replaced with the methionine-deficient DMEM medium supplied with 10% dialyzed FBS and various concentrations of methionine analogues. The cells were incubated for 24 h unless mentioned otherwise and then harvested. The transfection efficiency of the plasmids was confirmed by Western blotting using the following antibodies: *anti*-Flag (Sigma, Cat. No.: F3165); *anti*-G9a (Millipore, Cat. No.: 07-551); anti-GLP1 (Millipore, Cat. No.: 09-078; anti-MAT2A (Abcam, Cat. No.: ab77471). The Western blotting was performed as described before.[29]

Measurement of the Production of Hey-SAM (2c) within Living Cells. HEK293T cells were transfected with mock (empty pcDNA3 vector) or the MAT2A I117A plasmid and then incubated with different concentrations of Hey-Met **1c** according to the protocols described above. After 24 h incubation, the cells were harvested and lysed in ice-cold RIPA buffer (Sigma) containing 1× Complete EDTA-free protease inhibitor cocktail (Roche). The cell lysates were then mixed with an equal volume of 20% $HClO_4$. The samples were passed through a 3K centrifugal filter (Millipore) to remove the precipitated materials. The resultant flow-through was collected and resolved by reversed-phase HPLC (DELTA PAK C18

15 μm, 300 × 3.9 mm) by monitoring UV260 nm with a gradient of acetonitrile in aqueous trifluoroacetic acid (0.01%) from 0% to 10% in 15 min and then to 70% in 5 min at a flow rate of 1 mL/min. The resultant Hey-SAM **2c** was collected and confirmed by ESI-MS (Figure 3b, Figure S5 in the Supporting Information). To further quantify the amount of Hey-SAM **2c** generated within living cells, about 10^7 HEK293T cells that were transfected with the MAT2A I117A and then treated with 1 mM Hey-Met **1c** were lysed as described above. After removing the precipitated materials, the known amount of 5′-deoxy-methylthioadenosine (MTA) was added as the internal standard before injecting to HPLC. The peak area of Hey-SAM was integrated and compared to that of MTA to quantify the amount of Hey-SAM produced within the cells.

Alamar Blue Assay for Cell Viability. HEK293T cells (with or without transfection of MAT2A I117A plasmid) were resuspended in DMEM medium containing 10% FBS and then seeded into 96-well plates (100 μL/well) at a concentration of 10^5 cells/mL for an initial 12 h period for cell attachment. Subsequently, the medium was replaced with 100 μL of methionine-deficient DMEM medium containing the varied concentrations of Hey-Met **1c**. After incubating with the compound for 8 h, cell viability was determined by adding Alamar blue (Invitrogen, Cat. No.: DAL1100) into the culture medium at the final concentration of 10%, and the plate was returned to the incubator. Optical density of the plate was measured at the excitation wavelength of 530 nm and the emission wavelength at 590 nm with a standard spectrophotometer 4 h after adding Alamar blue. The results were presented as a percentage of the control without adding Hey-Met **1c**.

In-Gel Fluorescence of Proteome-Wide Substrates of G9a within Living Cells. HEK293T cells were transfected with the engineered MAT2A and/or G9a mutant plasmids and then treated with 1 mM Hey-Met **1c** for a varied period of time. The resultant cells were harvested and lysed in an ice-cold RIPA buffer containing 1× Complete EDTA-free protease inhibitor cocktail. After centrifugation, the supernatant was passed through the detergent removal spin column (Pierce, Cat. No.: 87778) and eluted with Tris buffer (100 mM Tris, pH = 8.0, 10% glycrol, 1 mM TCEP). 50 μg of cell lysates (protein concentration was determined by Bradford assay, Bio-Rad Laboratories) was subjected to CuAAC, followed by in-gel fluorescence as described previously.[30]

Pull-down and Acid Extraction of Histones in Cellular Contexts. HEK293T cells were transfected with the engineered MAT2A and G9a or GLP1 mutant plasmids and then treated with 1 mM Hey-Met (**1c**) as described above. The resultant cells were harvested and lysed in ice-cold RIPA buffer containing 1× Complete EDTA-free protease inhibitor cocktail. Into 2 mg of the lysates was added the CuAAC ligation cocktail (1 mM $CuSO_4$, 100 μM Tris [(1-benzyl-1*H*-1,2,3-triazol-4-yl)methyl]amine (TBTA), 2.5 mM Tris (2-carboxyethyl)phosphine hydrochloride (TCEP) and 200 μM azido−diazo−biotin as the final concentrations).[29,31] The mixture was further incubated for 1 h at ambient temperature (22 °C).[31] The reaction was quenched by the addition of 10 mL of cold methanol into each sample and kept at −80 °C overnight. Precipitated proteins were centrifuged at 3,000 rpm for 30 min, washed twice with 10 mL of cold methanol and dried for 20 min. The dried protein samples were redissolved in 400 μL of dilution buffer (50 mM triethylamine at pH = 7.4, 150 mM NaCl, 1× Complete EDTA-free protease inhibitor cocktail and 0.5% SDS) with gentle vortexing and sonication. For each sample, 50 μg of protein was spared as loading control of Western blotting, and the remaining samples were mixed with 50 μL of Streptavidin Sepharose High Performance beads (GE Healthcare) that were prewashed and resuspended in the dilution buffer, and rotated end-to-end at ambient temperature (22 °C) for 1 h. The samples were then washed once with PBS containing 0.2% SDS, twice with PBS and once with 250 mM ammonium bicarbonate buffer. The proteins were finally eluted for 30 min with 500 μL of elution buffer containing 25 mM sodium dithionite and 250 mM ammonium bicarbonate at ambient temperature (22 °C) and concentrated by Amicon Ultra centrifugal filters (Millipore). The eluted protein samples were then snap-frozen, lyophilized into powder and dissolved in 1× loading buffer (Biorad). These samples were resolved by SDS−PAGE and analyzed by Western blotting using *anti*-histone H3 antibody (Millipore, Cat. No.: 05-928) according to the previous protocol.[29] To extract core histones, HEK293T cells were first resuspended in 1× hypotonic lysis buffer (Sigma, Cat. No.: L9161) supplemented with 1× Complete EDTA-free protease inhibitor cocktail and incubated on ice for 15 min. To the resultant cell lysates was added NP-40 to a final concentration of 0.6%, followed by vigorous vortexing of the samples for 10 s. The samples were then centrifuged at 11000*g* at 4 °C for 10 min. The nuclear pellet was washed once in the ice-cold hypotonic buffer, and resuspended in 0.4 N H_2SO_4 and extracted at 4 °C overnight. After centrifuging the samples at 11000*g* at 4 °C for 10 min, the supernatant containing core histones were collected and resolved in 18% SDS−PAGE. The corresponding gel bands were excised and subjected to LC−MS/MS analysis as described previously.[13,17,29]

Native Chromatin Immunoprecipitation (ChIP) and Clickable Chromatin Enrichment (CliEn). For native chromatin immunoprecipitation (ChIP), the nuclei were isolated from 10^7 HET293T cells using 1× hypotonic lysis buffer (Sigma) as described above, resuspended in the digestion buffer (0.32 M sucrose, 50 mM Tris-HCl at pH = 7.5, 4 mM MgCl2, 1 mM CaCl2, 0.1 mM PMSF and 1× Complete EDTA-free protease inhibitor cocktail) and then digested with micrococcal nuclease (MNase, Sigma, Cat. No.: N3755). Here MNase's concentrations and digestion time were optimized for each set of experiments according to the reported protocol.[32] The MNase-mediated digestion was carried out for 10 min at 37 °C and stopped by the addition of EDTA to the final concentration of 5 mM. The resultant samples were then centrifuged at 10000*g* for 5 min, and the supernatant was collected as the S1 fraction. The remaining pellet was resuspended in 1 mL of lysis buffer (1 mM Tris-HCl, pH = 7.4, 0.2 mM EDTA, 0.2 mM PMSF and 1× Complete EDTA-free protease inhibitor cocktail) and dialyzed against the same buffer using 2K MWCO Slide-A-Lyzer Dialysis Cassette (Thermo Scientific) for 3 h at 4 °C. After dialysis, the samples were centrifuged at 10000*g* for 5 min, and the supernatant was collected as the S2 fraction. The soluble chromatin was prepared by combining the S1 and S2 fractions. With the samples, immunoprecipitation was carried out with anti-H3K9me2 antibody (Millipore, Cat. No.: 17-681) coupled with 100 μL of protein G magnetic beads (Millipore) at 4 °C overnight. The beads enriched with the target proteins were then washed sequentially with buffer A (50 mM Tris-HCl at pH = 7.5, 10 mM EDTA and 50 mM NaCl), buffer B (50 mM Tris-HCl at pH = 7.5, 10 mM EDTA and 100 mM NaCl) and buffer C (50 mM Tris-HCl at pH = 7.5, 10 mM EDTA, and 150 mM NaCl). The bound chromatin was eluted with 500 μL of elution buffer (20 mM Tris-HCl at pH = 7.5, 50 mM NaCl, 1× Complete EDTA-free protease inhibitor cocktail and 1% SDS) with agitation for 30 min at ambient temperature (22 °C). The chromatin samples were digested with Proteinase K (Sigma, Cat. No.: P2308) at 55 °C for 2 h and the DNA was purified by QIAquick PCR Purification columns (Qiagen) using buffer PB, and analyzed by quantitative PCR (qPCR) as described below.

For clickable chromatin enrichment (CliEn), the soluble chromatins, prepared above prior to the step of antibody immunoprecipitation, were subject to the CuAAC cocktail (1 mM CuSO4, 100 μM Tris [(1-benzyl-1*H*-1,2,3-triazol-4-yl)methyl]amine (TBTA), 2.5 mM Tris (2-carboxyethyl)phosphine hydrochloride (TCEP) and 200 μM azido−diazo−biotin as the final concentrations) for 1 h at ambient temperature (22 °C) with rotation. Into the mixture was added 100 μL of streptavidin beads, which were prewashed and resuspended in the incubation buffer (20 mM Tris-HCl at pH = 7.5, 50 mM NaCl and 1× Complete EDTA-free protease inhibitor cocktail). The resultant sample was mixed gently with a rotator for another 3 h at 4 °C. The streptavidin beads were then sequentially washed with 10 mL of PBS containing 0.1% SDS and the 2× incubation buffer (20 mM Tris-HCl at pH = 7.5, 50 mM NaCl and 1× Complete EDTA-free protease inhibitor cocktail). The chromatins were eluted with 500 μL of elution buffer (25 mM sodium dithionite, 1% SDS, 20 mM Tris-HCl, pH = 7.5, 50 mM NaCl and 1× Complete EDTA-free protease inhibitor cocktail) with agitation for 30 min at

ambient temperature (22 °C). The eluates were digested with Proteinase K at 55 °C for 2 h, and the DNA was purified by QIAquick PCR Purification columns (Qiagen) using buffer PB, and analyzed by quantitative PCR (qPCR) as described below. The bound and input DNA samples from native chromatin immunoprecipitation (ChIP) or clickable chromatin enrichment (CliEn) were analyzed by qPCR with SYBR Green PCR Master Mix (Applied Biosystems) using the ABI Prism 7500 fast real-time PCR machine. Primers for qPCR are provided in Table S1 in the Supporting Information. Relative ChIP-qPCR values are presented as the fold of changes versus the control groups (without transfection of native G9a or GLP1); CliEn-qPCR data are presented similarly as the fold of changes versus the control groups (without transfection of MAT2A I117A, G9a Y1154A or GLP1 Y1211A variants).

Samples and Data Process for CliEn-seq. CliEn samples were prepared for sequencing using Illumina TruSeq DNA Sample Preparation Kit according to the standard preparation protocol (http://www.illumina.com/) with some modifications. The CliEn DNA and input DNA concentrations were first measured by Bioanalyzer (Agilent) (for cells transfected with MAT2A I117A, CliEn DNA 2.44 ng, input DNA 2078.75 ng; for cells cotransfected with MAT2A I117A and G9a Y1154A, CliEn DNA 115.44 ng, input DNA 2058.70 ng; for cells cotransfected with MAT2A I117A and GLP1 Y1211A, CliEn DNA 84.61 ng, input DNA 2305.15 ng) and are presented in Figure 4b. Next, ∼5 ng of the CliEn DNA or input DNA was used for library preparation and a 1:10 dilution of the DNA adapters was ligated. DNA fragments were then amplified with PCR Primer Cocktail (6 cycles), and 1/10 of the PCR product was checked on the Agilent Bioanalyzer. The purified DNA libraries were diluted to 10 nM for loading on the flow cell. Sequencing service was performed on an Illumina HiSeq 2000 sequencer according to the standard Illumina protocol resulting in ∼15 million quality-filtered sequences of length 75/75 per sample. CliEn-seq reads were aligned to the reference human genome (hg19, NCBI Build 37) using the BWA program,[33] and the reads mapped to multiple locations were filtered out with only one position saved. The sequence results were processed, normalized by total reads and displayed using the GenPlay tool. The Illumina HiSeq data have been deposited into GEO (Accession Number GSE42792). To generate the CliEn-seq read density profiles, we used the ChIPseeqer-2.0.[34] A read density matrix was generated with the average number of reads in 10 bp bins for a window of ±2 kb around the transcription start site (TSS) or the transcription end site (TES) of the 35 selected genes (Table S2 in the Supporting Information). The read density plot was created with the mean value per bin in the matrix.

■ ASSOCIATED CONTENT

Supporting Information

Additional procedures, synthetic methods and characterizations for the precursors of methionine analogues, NMR spectra and supplementary figures. This material is available free of charge via the Internet at http://pubs.acs.org.

■ AUTHOR INFORMATION

Corresponding Author

luom@mskcc.org

Author Contributions

[§]These authors made equal contribution.

Notes

The authors declare no competing financial interest.

■ ACKNOWLEDGMENTS

We thank Drs. Min, Huang, Oppermann and Schramm for plasmids; Genomics Core Laboratory and Dr. Agnes Viale at MSKCC for DNA sequencing service; NIGMS (1R01GM096056), the NIH Director's New Innovator Award Program (1DP2-OD007335), the V Foundation for Cancer Research, March of Dimes Foundation, Starr Cancer Consortium, and the Alfred W. Bressler Scholars Endowment Fund for financial support.

■ REFERENCES

(1) Schubert, H. L.; Blumenthal, R. M.; Cheng, X. *Trends Biochem. Sci.* **2003**, *28*, 329.
(2) Greer, E. L.; Shi, Y. *Nat. Rev. Genet.* **2012**, *13*, 343.
(3) Luo, M. *ACS Chem. Biol.* **2012**, *7*, 443.
(4) Geiman, T. M.; Robertson, K. D. *J. Cell. Biochem.* **2002**, *87*, 117.
(5) Clapier, C. R.; Cairns, B. R. *Annu. Rev. Biochem.* **2009**, *78*, 273.
(6) Fritsch, L.; Robin, P.; Mathieu, J. R.; Souidi, M.; Hinaux, H.; Rougeulle, C.; Harel-Bellan, A.; Ameyar-Zazoua, M.; Ait-Si-Ali, S. *Mol. Cell* **2010**, *37*, 46.
(7) Garcia-Cao, M.; O'Sullivan, R.; Peters, A. H.; Jenuwein, T.; Blasco, M. A. *Nat. Genet.* **2004**, *36*, 94.
(8) Kim, K. C.; Geng, L.; Huang, S. *Cancer Res.* **2003**, *63*, 7619.
(9) Xu, P. F.; Zhu, K. Y.; Jin, Y.; Chen, Y.; Sun, X. J.; Deng, M.; Chen, S. J.; Chen, Z.; Liu, T. X. *Proc. Natl. Acad. Sci. U. S. A.* **2010**, *107*, 2521.
(10) Komoto, J.; Yamada, T.; Takata, Y.; Markham, G. D.; Takusagawa, F. *Biochemistry* **2004**, *43*, 1821.
(11) Lin, Q.; Jiang, F.; Schultz, P. G.; Gray, N. S. *J. Am. Chem. Soc.* **2001**, *123*, 11608.
(12) Shinkai, Y.; Tachibana, M. *Genes Dev.* **2011**, *25*, 781.
(13) Islam, K.; Zheng, W.; Yu, H.; Deng, H.; Luo, M. *ACS Chem. Biol.* **2011**, *6*, 679.
(14) Cantoni, G. *J. Am. Chem. Soc.* **1952**, *74*, 2942.
(15) Catoni, G. L. *J. Biol. Chem.* **1953**, *204*, 403.
(16) Bedford, M. T.; Clarke, S. G. *Mol. Cell* **2009**, *33*, 1.
(17) Wang, R.; Zheng, W.; Yu, H.; Deng, H.; Luo, M. *J. Am. Chem. Soc.* **2011**, *133*, 7648.
(18) Melnyk, S.; Pogribna, M.; Pogribny, I. P.; Yi, P.; James, S. *J. Clin. Chem.* **2000**, *46*, 265.
(19) Yang, Y. Y.; Ascano, J. M.; Hang, H. C. *J. Am. Chem. Soc.* **2010**, *132*, 3640.
(20) Couture, J. F.; Collazo, E.; Ortiz-Tello, P. A.; Brunzelle, J. S.; Trievel, R. C. *Nat. Struct. Mol. Biol.* **2007**, *14*, 689.
(21) Kruidenier, L.; Chung, C. W.; Cheng, Z.; Liddle, J.; Che, K.; Joberty, G.; Bantscheff, M.; Bountra, C.; Bridges, A.; Diallo, H.; Eberhard, D.; Hutchinson, S.; Jones, E.; Katso, R.; Leveridge, M.; Mander, P. K.; Mosley, J.; Ramirez-Molina, C.; Rowland, P.; Schofield, C. J.; Sheppard, R. J.; Smith, J. E.; Swales, C.; Tanner, R.; Thomas, P.; Tumber, A.; Drewes, G.; Oppermann, U.; Patel, D. J.; Lee, K.; Wilson, D. M. *Nature* **2012**, *488*, 404.
(22) Ling, B. M.; Bharathy, N.; Chung, T. K.; Kok, W. K.; Li, S.; Tan, Y. H.; Rao, V. K.; Gopinadhan, S.; Sartorelli, V.; Walsh, M. J.; Taneja, R. *Proc. Natl. Acad. Sci. U. S. A.* **2012**, *109*, 841.
(23) Kubicek, S.; O'Sullivan, R. J.; August, E. M.; Hickey, E. R.; Zhang, Q.; Teodoro, M. L.; Rea, S.; Mechtler, K.; Kowalski, J. A.; Homon, C. A.; Kelly, T. A.; Jenuwein, T. *Mol. Cell* **2007**, *25*, 473.
(24) Rathert, P.; Dhayalan, A.; Murakami, M.; Zhang, X.; Tamas, R.; Jurkowska, R.; Komatsu, Y.; Shinkai, Y.; Cheng, X.; Jeltsch, A. *Nat. Chem. Biol.* **2008**, *4*, 344.
(25) Rea, S.; Eisenhaber, F.; O'Carroll, D.; Strahl, B. D.; Sun, Z. W.; Schmid, M.; Opravil, S.; Mechtler, K.; Ponting, C. P.; Allis, C. D.; Jenuwein, T. *Nature* **2000**, *406*, 593.
(26) Martin, C.; Zhang, Y. *Nat. Rev. Mol. Cell. Biol.* **2005**, *6*, 838.
(27) Collas, P. *Mol. Biotechnol.* **2010**, *45*, 87.
(28) Dalhoff, C.; Lukinavicius, G.; Klimasauskas, S.; Weinhold, E. *Nat. Chem. Biol.* **2006**, *2*, 31.
(29) Islam, K.; Bothwell, I.; Chen, Y.; Sengelaub, C.; Wang, R.; Deng, H.; Luo, M. *J. Am. Chem. Soc.* **2012**, *134*, 5909.
(30) Bothwell, I. R.; Islam, K.; Chen, Y.; Zheng, W.; Blum, G.; Deng, H.; Luo, M. *J. Am. Chem. Soc.* **2012**, *134*, 14905.
(31) Yang, Y. Y.; Grammel, M.; Raghavan, A. S.; Charron, G.; Hang, H. C. *Chem. Biol.* **2010**, *17*, 1212.

(32) Wagschal, A.; Delaval, K.; Pannetier, M.; Arnaud, P.; Feil, R. *CSH Protoc.* 2007, 2007, pdb prot4767.
(33) Li, H.; Durbin, R. *Bioinformatics* **2009**, *25*, 1754.
(34) Giannopoulou, E. G.; Elemento, O. *BMC Bioinformatics* **2011**, *12*, 277.